Peer-reviewed version available at *Int. J. Mol. Sci.* **2019**, *20*, 4437; doi:10.3390/ijms20184437

OsWRKY5 Promotes Rice Leaf Senescence by Upregulating Senescence-Associated *NAC* Genes and Abscisic Acid Biosynthesis

Taehoon Kim [1,3], Kiyoon Kang [1,3], Suk-Hwan Kim [1], Gynheung An [2] and Nam-Chon Paek [1,*]

[1] Department of Plant Science, Plant Genomics and Breeding Institute, Research Institute of Agriculture and Life Sciences, Seoul National University, Seoul 08826, Korea; taehoonkim7@snu.ac.kr (T.K.); kykang7408@snu.ac.kr (K.K.); sukhwan0819@snu.ac.kr (S.-H. K.)

[2] Crop Biotech Institute and Graduate School of Biotechnology, Kyung Hee University, Yongin 17104, Korea; genean@khu.ac.kr (G.A.).

[3] These authors contributed equally to this work.

* Corresponding author: ncpaek@snu.ac.kr (N.-C. P.); Tel.: +82-2-880-4543; Fax: +82-2-877-4550

Abstract: The onset of leaf senescence is triggered by external cues and internal factors such as phytohormones and signaling pathways involving transcription factors (TFs). Abscisic acid (ABA) strongly induces senescence and endogenous ABA levels are finely tuned by many senescence-associated TFs. Here, we report on the regulatory function of the senescence-induced TF OsWRKY5 TF in rice (*Oryza sativa*). *OsWRKY5* expression was rapidly upregulated in senescing leaves, especially in yellowing sectors initiated by aging or dark treatment. A T-DNA insertion activation-tagged *OsWRKY5*-overexpressing mutant (termed *oswrky5-D*) promoted leaf senescence under natural and dark-induced senescence (DIS) conditions. By contrast, a T-DNA insertion *oswrky5*-knockdown mutant (termed *oswrky5*) retained leaf greenness during DIS. Reverse-transcription quantitative PCR (RT-qPCR) showed that *OsWRKY5* upregulates the expression of genes controlling chlorophyll degradation and leaf senescence. Furthermore, RT-qPCR and yeast one-hybrid analysis demonstrated that OsWRKY5 indirectly upregulates the expression of senescence-associated *NAC* genes including *OsNAP* and *OsNAC2*. Precocious leaf yellowing in the *oswrky5-D* mutant might be caused by elevated endogenous ABA concentrations

resulting from upregulated expression of ABA biosynthesis genes *OsNCED3*, *OsNCED4*, and *OsNCED5*, indicating that OsWRKY is a positive regulator of ABA biosynthesis during leaf senescence. Furthermore, *OsWRKY5* expression was significantly suppressed by ABA treatment, indicating negative feedback regulation of *OsWRKY5* expression by ABA. *OsWRKY5* is a positive regulator of leaf senescence that upregulates senescence-induced *NAC* genes leading to expression of ABA biosynthesis and chlorophyll degradation genes.

Keywords: rice; leaf senescence; abscisic acid (ABA); OsWRKY; NAC

1. Introduction

Leaf senescence is the final stage of plant development and involves diverse molecular and cellular processes such as degradation of chlorophylls and macromolecules, and remobilization of nutrients into newly developing or storage organs through expression of senescence-associated genes (SAGs). The onset of leaf senescence begins with chlorophyll degradation and proceeds to hydrolysis of macromolecules (proteins, lipids, and nucleic acids); this is followed by cell death [1-3].

Genetic studies have revealed the contribution of chlorophyll catabolic enzymes to sequential reactions of chlorophyll degradation. The STAY-GREEN (SGR) protein is a magnesium (Mg)-dechelatase, which produces pheophytin *a* by removing Mg from chlorophyll *a* [4, 5]. Thus, functional deficiency of SGR orthologs leads to a strong stay-green phenotype in diverse plant species including *Arabidopsis thaliana* [6], rice (*Oryza sativa*) [4], pea (*Pisum sativum*) [7], tomato (*Solanum lycopersicum*), bell pepper (*Capsicum annuum*) [8], and soybean (*Glycine max*) [9]. Failure to convert pheophytin *a* to pheophorbide *a* due to mutation of *NON-YELLOW COLORING3* (*NYC3*), encoding an α/β hydrolase-fold family protein, delays leaf senescence during dark-induced senescence (DIS) [10]. Knockdown of rice *pheophorbide a oxygenase* (*OsPAO*) leads to accumulation of pheide *a* and prolongs leaf greenness during dark incubation [11]. SAGs identified during leaf senescence in rice encode putative proteins involved in metabolic programing [12]; *Osh36* and *Osl85* encode an aminotransferase and isocitrate lyase, which participate in amino acid and fatty acid metabolism, respectively.

Leaf senescence generally occurs in an age-dependent manner, but it can be affected by internal and environmental factors such as phytohormones, pathogen infection, extreme temperatures, salt, drought, nutrient deficiency, and shading [1, 13-15]. Abscisic acid (ABA) participates in multiple aspects of plant development including leaf senescence, seed germination, stomatal closure, and root development [16-18]. Specifically, expression of ABA biosynthetic genes such as those encoding 9′-*cis*-epoxycarotenoid dioxygenases (NCEDs) is induced by leaf senescence, elevating endogenous ABA levels in Arabidopsis leaves [19, 20]. Increased levels of endogenous ABA can activate chlorophyll degradation pathways mediated by senescence-associated transcription factors (TFs) [21-24]. For instance, ABA induces the expression of the genes encoding ABA-RESPONSIVE ELEMENT (ABRE)-BINDING TRANSCRIPTION FACTOR 2 (ABF2), ABF3, and ABF4, which directly bind to the *SGR1* promoter, accelerating chlorophyll degradation in Arabidopsis leaves [21]. In rice, ABA-promoted expression of *OsNAP* directly upregulates chlorophyll degradation genes (CDGs) such as *SGR*, *NYC1*, *NYC3*, and *RCCR1*, leading to early leaf senescence [25].

The WRKY TFs participate in various biological processes such as biotic and abiotic stress, seed development, seed dormancy, and germination [26]. Genome-wide analyses have revealed that many WRKY genes are strongly induced by leaf senescence [27, 28], suggesting that WRKY TFs are involved in regulating leaf senescence. Following identification of AtWRKY6 as a regulator of leaf senescence [29], other WRKY TFs regulating leaf senescence have been functionally characterized. For example, mutation of Arabidopsis *AtWRKY53* confers a delayed leaf senescence phenotype by specifically altering regulation of its target genes [30]. Overexpression of *AtWRKY22*, a target gene of AtWRKY53, accelerates leaf senescence [31]. AtWRKY54 and AtWRKY70 act as negative regulators of leaf senescence by interacting independently with WRKY30 [32]. AtWRKY45 mediates gibberellic acid (GA)-induced leaf senescence by interacting with a DELLA protein, RGL1 [33]. AtWRKY75 increases salicylic acid (SA) and H_2O_2 levels by activating *SID2* and repressing *CAT2*, respectively, resulting in early leaf senescence [34]. Heterologous expression of rice *OsWRKY23* promotes leaf senescence in Arabidopsis [35]. Rice OsWRKY42 induces reactive oxygen species (ROS) by directly downregulating the expression of *OsMT1d* encoding metallothionein protein and thereby promoting leaf senescence [36]. Unlike Arabidopsis WRKY TFs involved in the regulation of leaf

senescence; however, few OsWRKY TFs have been identified as functioning in the execution of leaf senescence.

In this study, we found that *OsWRKY5* expression is upregulated at the onset of leaf senescence. The *OsWRKY5*-overexpressing *oswrky5-D* mutation promoted leaf yellowing under aging and dark treatment, while an *oswrky5*-knockdown mutant exhibited a delayed senescence phenotype. Reverse-transcription quantitative PCR (RT-qPCR) analysis suggested that CDGs and SAGs were upregulated by senescence-induced OsWRKY5. Furthermore, OsWRKY5 indirectly regulated the expression of senescence-associated *NAC* (*senNAC*) genes such as *OsNAP* and *OsNAC2*, which are upstream regulators of CDGs and SAGs. *OsWRKY5* elevated endogenous ABA levels by upregulating the expression of ABA biosynthetic genes. Our results thus provide evidence that OsWRKY5 acts as a positive regulator of leaf senescence in rice.

2. Results

2.1. Characterization of OsWRKY5

OsWRKY5 (Os05g04640), a member of rice WRKY TF family, consists of six exons with 1509 bp of open reading frame in 5379 bp of genomic DNA. *OsWRKY5* is predicted to encode a 502 amino acid protein with a molecular mass of 52.3 kDa. The WRKY domain of OsWRKY5 has a single consensus motif (WRKYGQK) and a zinc-finger C_2H_2 motif ($Cx_5Cx_{23}HxH$), indicating that OsWRKY5 belongs to the group II WRKY TF family [37]. From sequence alignment of WRKY domains between OsWRKY5 and group II *Arabidopsis thaliana* WRKY (AtWRKY) proteins, we found that the domain sequences of OsWRKY5 are quite similar to those of AtWRKY6 and AtWRKY47, members of the subgroup IIb AtWRKY TF family (**Figure S1**). To examine the subcellular localization of OsWRKY5, we transiently expressed the *35S::YFP-OsWRKY5* construct in onion epidermal cells. The fluorescent signal of YFP-OsWRKY5 fusions was observed exclusively in nuclei (**Figure S2**), indicating that OsWRKY5 is a nuclear-localized protein.

2.2. OsWRKY5 Is Upregulated during Leaf Senescence

To examine the spatial expression of *OsWRKY5*, we investigated transcript levels of *OsWRKY5* in rice organs including root, culm, leaf blade, leaf sheath, and panicle at the

reproductive stage (**Figure 1a**). *OsWRKY5* was preferentially expressed in the leaf blade and leaf sheath. Previous transcriptome analysis [28] showed upregulation of 47 rice WRKY TFs including *OsWRKY5* in flag leaves during natural senescence (NS). Therefore, we determined age-dependent changes in *OsWRKY5* expression in flag leaves of wild-type (WT; *japonica* cultivar 'Dongjin') rice grown in a paddy field under natural long-day (NLD) conditions (>14 h light/day). While *OsWRKY5* was constitutively expressed in developing leaves at the vegetative stage, *OsWRKY5* expression was dramatically upregulated in senescing leaves at the reproductive stage (**Figure 1b**). In addition, *OsWRKY5* expression gradually increased in detached leaves of four-week-old WT leaves during DIS (**Figure 1c**). We further found that *OsWRKY5* transcripts accumulated in the yellowing sector (region **c**) more than in the green sector (region **a**) of senescing flag leaves (**Figure 1d**). These results suggest that *OsWRKY5* is involved in the onset and progression of leaf senescence in rice.

2.3. OsWRKY5 Positively Regulates the Progression of Leaf Senescence

To examine the function of *OsWRKY5* in leaf senescence, we identified activation-tagged and loss-of-function mutants. To this end, we obtained two independent T-DNA insertion lines (PFG_3A-15928 and PFG_3A-06060) from the RiceGE database (http://signal.salk.edu/cgi-bin/RiceGE) in which each T-DNA fragment with an activation tag (4× 35S promoter) was integrated into the promoter region of *OsWRKY5* (**Figure 2a**). To verify the expression levels of *OsWRKY5* in these mutant lines, we measured *OsWRKY5* expression levels in detached leaves of four-week-old mutant plants during DIS. RT-qPCR showed that *OsWRKY5* transcripts accumulated to high levels in PFG_3A-15928 compared to the WT due to the activation-tagged T-DNA insertion; by contrast, in PFG_3A-06060, the T-DNA insertion in the promoter region of *OsWRKY5* reduced expression of *OsWRKY5* (**Figure 2b,c**). These results indicate that PFG_3A-15928 and PFG_3A-06060 are dominant activation and recessive knockdown mutants, respectively (hereafter termed *oswrky5-D* and *oswrky5*, respectively). To confirm this, we further investigated the *OsWRKY5* expression in leaf blade, leaf sheath, and root separated from WT and mutant lines grown in paddy soil for three weeks. Similar to expression patterns of *OsWRKY5* shown in detached leaves during DIS (**Figure 2b,c**), *OsWRKY5* transcripts highly accumulated in all tissues of *oswrky5-D* compared with the WT, while they were significantly lower in *oswrky5* than in the WT (**Figure 2d,e**).

Peer-reviewed version available at Int. J. Mol. Sci. 2019, 20, 4437; doi:10.3390/ijms20184437

To determine the phenotypic difference between WT and mutant lines during DIS, we next incubated detached leaves of three-week-old WT, *oswrky5-D*, and *oswrky5* plants in 3 mM MES buffer (pH 5.8) at 28°C under complete darkness. While *oswrky5-D* showed accelerated leaf yellowing compared with the WT, the *oswrky5* leaves retained their green color longer than the WT leaves (**Figure 3a,b**). Consistent with the leaf color, the total chlorophyll content of *oswrky5-D* was less than that of the WT after DIS, whereas *oswrky5* maintained higher total chlorophyll levels during DIS compared with the WT (**Figure 3c,d**).

In senescing leaves, chlorophylls are sequentially degraded by chlorophyll-degrading enzymes including SGR [4], NYC3 [10], and OsPAO [11]. Many other SAGs are also upregulated during DIS in rice, with products identified as seed imbibition protein (Osh69), glyoxylate aminotransferase (Osh36), and isocitrate lyase (Osl85) [12]. We therefore measured transcript levels of CDGs and SAGs in detached leaves of three-week-old WT, *oswrky5-D*, and *oswrky5* plants under DIS conditions as shown in Fig. 2. RT-qPCR analysis revealed that expression of CDGs and SAGs was upregulated in *oswrky5-D* after 4 days of dark incubation (DDI) (**Figure 4a–f**) but downregulated in *oswrky5* after 5 DDI when compared with the WT (**Figure 4g–l**). These results demonstrate that *OsWRKY5* promotes the onset and progression of leaf senescence by upregulating expression of CDGs and SAGs.

To further examine how *OsWRKY5* overexpression affects leaf senescence during vegetative and reproductive stages, we monitored age-dependent leaf yellowing in WT and *oswrky5-D* plants grown under NLD conditions (>14 h daylight) in the field (37° N latitude, Suwon, South Korea). While there was no significant difference in leaf color between the WT and *oswrky5-D* until heading (**Figure 5a**), the leaves of *oswrky5-D* showed a precocious leaf senescence phenotype at 40 days after heading (DAH) (**Figure 5b,c**). The SPAD value, a parameter for leaf greenness, indicated lower levels of green pigments in flag leaves of *oswrky5-D* compared with the WT at 24 DAH (**Figure 5d**). Leaf greenness is closely linked to photosynthetic capacity [38, 39]. Thus, reduced SPAD value led to a relatively lower *Fv/Fm* ratio (efficiency of photosystem II) in *oswrky5*-D than in WT at 24 DAH (**Figure 5e**). Similar to expression patterns of CDGs and SAGs during DIS, CDG and SAG transcripts were more abundant in the senescing flag leaves of *oswrky5-D* than in those of WT at 40 DAH (**Figure 5f**). These results indicate that OsWRKY5 acts as a positive regulator of leaf senescence during both NS and DIS.

2.4. OsWRKY5 Upregulates SenNAC Genes

Previous studies have shown that senNACs including OsNAP and OsNAC2 promote leaf senescence by upregulating expression of CDGs and SAGs [25, 40]. To determine whether *OsWRKY5* participates in NAC TF-mediated senescence pathways, we examined the expression levels of *OsNAP* and *OsNAC2* in detached leaves of WT, *oswrky5-D*, and *oswrky5* under DIS conditions. RT-qPCR showed that compared with the WT, in *oswrky5* the expression levels of *OsNAP* and *OsNAC2* were higher during dark incubation (**Figure 6a,b**), while they were downregulated at 0 and 4 DDI compared with the WT (**Figure 6c,d**). These results suggest that OsWRKY5 acts upstream of the OsNAP and OsNAC2 regulatory pathways to promote leaf senescence.

WRKY TFs regulate the transcription of their target genes by recognizing a consensus *cis*-element, the so-called W-box [26]. The W-box has been generally defined as 5′-TTGAC(C/T)-3′ with an invariant TGAC core sequence essential for WRKY binding [37, 41]. Since repetitive TGAC sequences enhance WRKY binding efficiency, we searched for the TGAC core sequence within 2 kb upstream of the transcriptional initiation sites of *OsNAP* and *OsNAC2*, and found two regions (–1001 ~ –765 and –657 ~ –575) in the promoter of *OsNAP* and five regions (–1760 ~ –1574, –1411 ~ –1309, –1135 ~ –1021, –660 ~ –480, and –352 ~ –98) in the promoter of *OsNAC2* (**Figure 6e**). To investigate whether the OsWRKY5 TF directly binds to the promoters of *OsNAP* and *OsNAC2*, we performed yeast one-hybrid assays. However, we could not find any difference between GAL4AD and GAL4AD-OsWRKY5 by measuring β-galactosidase activity of *lacZ* reporter genes, indicating that OsWRKY5 does not bind directly to the promoter of *OsNAP* or *OsNAC2* (**Figure 6f**).

Previous studies have reported that the microRNA osa-miR164b is closely associated with the post-transcriptional regulation of *OsNAC2*, resulting in reduction of *OsNAC2* mRNA levels [42, 43]. To examine whether OsWRKY5 regulates endogenous levels of osa-miR164b during DIS, we determined the expression of osa-miR164b in detached leaves of three-week-old WT, *oswrky5-D*, and *oswrky5* plants using stem-loop RT-PCR analysis. This revealed no difference in the levels of osa-miR164b among genotypes (**Figure S3**), suggesting that *OsWRKY5* indirectly regulates *OsNAC2* independent of osa-miR164b.

2.5. OsWRKY5 Is Involved in Negative Feedback Regulation of ABA Biosynthesis

Among phytohormones affecting the onset and progression of leaf senescence [2], ABA activates senescence-associated regulatory pathways, leading to acceleration of leaf senescence [44]. Genetic studies have revealed that the endogenous ABA concentration is delicately controlled by senNACs such as OsNAP and OsNAC2 [25, 40]. Considering that OsWRKY5 upregulated the expression of *OsNAP* and *OsNAC2*, we speculated that OsWRKY5 is mainly involved in regulating ABA biosynthesis. Indeed, the endogenous ABA concentration was significantly higher in leaves of three-week-old *oswrky5-D* plants than in those of the WT **(Figure 7a)**. RT-qPCR analysis showed that ABA biosynthesis genes including *OsNCED3*, *OsNCED4*, and *OsNCED5* were significantly upregulated in *oswrky5-D* leaves compared with the WT (**Figure 7b**). This strongly suggests that the early leaf senescence of *oswrky5-D* is mainly due to an increase in ABA biosynthesis after heading.

To investigate whether phytohormones affect the expression of *OsWRKY5*, we next measured the expression of *OsWRKY5* in ten-day-old WT seedlings exogenously treated with epibrassinolide (BR), gibberellic acid (GA), indole-3-acetic acid (IAA), 6-benzylaminopurine (6-BA), salicylic acid (SA), methyl jasmonic acid (MeJA), ABA, or 1-aminocyclopropane-1-carboxylic acid (ACC). RT-qPCR showed that *OsWRKY5* expression was significantly reduced by MeJA and ABA treatments (**Figure 7c**), indicating that excessive levels of ABA decrease the expression of *OsWRKY5* in a negative feedback manner.

3. Discussion

3.1. OsWRKY5 Promotes Leaf Yellowing during NS and DIS

We found that *OsWRKY5* participates in the ABA-mediated regulatory pathways of leaf senescence. *OsWRKY5* was expressed in leaves and its transcription was activated by aging and dark treatment (**Figure 1b,c**). The WRKY domain of OsWRKY5 has the highest amino acid similarity to that of AtWRKY6 (**Figure S1**). Similar to the early leaf senescence phenotype of *AtWRKY6*-OX in Arabidopsis [29], the progression of leaf senescence was much faster in the *oswrky5-D* mutant than in WT plants under NS and DIS conditions. (**Figures 3 and 5**), and the *oswrky5* knockdown mutant showed markedly delayed leaf senescence (**Figure 3**).

Many senescence-induced TFs directly or indirectly regulate expression of their target genes, including CDGs, SAGs, and other senescence-associated TFs. OsNAP directly binds to the

promoters of *SGR*, *NYC1*, *NYC3*, *RCCR1*, and *Osl57* (encoding a putative 3-ketoacyl-CoA thiolase). OsNAP also indirectly regulates the expression of *Osh36* and *Osh69*, whose amino acid sequences are quite similar to those of *Arabidopsis thaliana* aminotransferase and *Brassica oleracea* seed imbibition protein, respectively [25]. OsNAC2 enhances chlorophyll degradation by directly interacting with the promoters of *SGR* and *NYC3* [40]. We therefore speculate that *OsWRKY5* upregulates the expression of CDGs and SAGs by regulating senNACs. Upregulation of *OsNAP* and *OsNAC2* was observed in *oswrky5-D*, resulting in early leaf yellowing (**Figures 4 and 5**). However, OsWRKY5 does not bind to the promoter regions of *OsNAP* and *OsNAC2* despite the presence of repetitive TGAC core sequences (**Figure 6e,f**), suggesting that it indirectly regulates expression of these genes.

WRKY TFs can physically interact with other TFs involved in leaf senescence. For example, Besseau et al. (2012) showed that expression of Arabidopsis *WRKY30*, *WRKY53*, *WRKY54*, and *WRKY70* is induced during leaf senescence and WRKY53, WRKY54, and WRKY70 interact independently with WRKY30 in yeast two-hybrid assays [32]. In Arabidopsis, WRKY45 functions in GA-mediated leaf senescence by interacting with the DELLA protein RGA-LIKE1 (RGL1) characterized as a repressor of GA signaling [33]. Recently, TT2, a MYB family member, was identified as an interacting partner of WRKY27 in upland cotton (*Gossypium hirsutum* L.) [45]. Therefore, exploring the possible interaction networks of the OsWRKY5 TF in the regulation of senNACs should provide more insight into the mechanism of leaf senescence.

3.2. OsWRKY5 Mediates ABA-Induced Leaf Senescence

ABA promotes the onset and progression of leaf senescence [46]. Thus, endogenous ABA levels are elevated by upregulation of ABA biosynthesis genes during leaf senescence, promoting further ABA-induced leaf senescence [44, 47]. Arabidopsis *9-CIS-EPOXYCAROTENOID DIOXYGENASE* (*NCED*) genes, encoding a rate-limiting enzyme in ABA biosynthesis, are upregulated during NS [19, 48]. Dark incubation induces expression of *OsNCED3* in rice leaves [49], and overexpression of *OsNCED3* accelerates leaf yellowing in rice during dark incubation. *NAP* increases ABA biosynthesis by directly upregulating transcription of *ABSCISIC ALDEHYDE OXIDASE3* (*AAO3*), leading to chlorophyll degradation during dark incubation in Arabidopsis [20]. In rice, although transcription of ABA biosynthesis genes, such as *OsNCED1*, *OsNCED3*, *OsNCED4*, and *OsZEP*, is inhibited by OsNAP, the functional ortholog of Arabidopsis NAP,

overexpression of *OsNAP* leads to precocious leaf senescence by directly regulating CDGs and SAGs [25]. *OsNAC2* elevates endogenous ABA content by directly binding to the promoters of *OsNCED3* and *OsZEP*, thereby promoting leaf senescence [40]. Transgenic Arabidopsis plants heterologously expressing foxtail millet (*Setaria italica*) *NAC1* (*SiNAC1*) show enhanced transcription of ABA biosynthesis genes, *NCED2* and *NCED3*, resulting in early leaf senescence [50]. Although ABA signaling pathways mediated by WRKY TFs are involved in multiple aspects of plant development including leaf senescence [51], molecular evidence for WRKY TF involvement in ABA biosynthesis is limited. In this study, we found that OsWRKY5 upregulates transcription of ABA biosynthesis genes, *OsNCED3*, *OsNCED4*, and *OsNCED5* (**Figure 7b**), suggesting that OsWRKY5 functions in the promotion of leaf senescence by increasing ABA biosynthesis (**Figure 7a**). Furthermore, based on the involvement of *OsWRKY5* in *OsNAC2* expression (**Figure 6b,d**), *OsWRKY5* probably activates an *OsNAC2*-mediated ABA biosynthetic pathway (**Figure 8**).

Plants have developed several regulatory mechanisms to restore ABA homeostasis during leaf senescence. For example, in tomato, *NAP2* directly regulates expression of genes regulating ABA biosynthesis (*NCED1*) and ABA degradation (*CYP707A2*) to establish ABA homeostasis during leaf senescence [52]. ABA-induced *OsNAP* represses the accumulation of endogenous ABA in rice, indicating that *OsNAP* participates in a negative feedback mechanism on ABA biosynthesis [25]. Expression of *OsNAC2* is differentially regulated by ABA concentration; *OsNAC2* expression is upregulated by 20 μM ABA, but inhibited by ABA concentrations over 40 μM [40]. Because the expression of *OsWRKY5* is reduced by excessive ABA treatment (**Figure 7c**), it is highly possible that *OsWRKY5* transcription is repressed by excessive concentrations of ABA via a negative feedback regulatory mechanism.

4. Experimental Section

4.1. Plant Materials, Growth Conditions, and Experimental Treatments

The *Oryza sativa japonica* cultivar ‘Dongjin’ (parental line), and the *oswrky5-D* and *oswrky5* mutants were grown in a growth chamber under LD conditions (14 h light at 28°C/10 h dark at 25°C) and in a rice paddy field under NLD conditions (≥14 h sunlight/day, 37°N latitude) in Seoul, Republic of Korea. The T-DNA insertion activation-tagged *oswrky5-D* and knockdown *oswrky5*

mutants were obtained from the Crop Biotech Institute at Kyung Hee University, Republic of Korea [53, 54].

For dark treatment, detached leaves of rice plants grown in the growth chamber for 3 weeks were incubated in 3 mM 2-(N-morpholino)ethanesulfonic (MES) buffer (pH 5.8) with the abaxial side up at 28°C in complete darkness. To detect *OsWRKY5* transcript levels under various hormone treatments, WT seeds were sterilized with 70% ethanol and 2% NaClO, and then germinated and grown on half-strength Murashige and Skoog (0.5X MS, Duchefa, The Netherlands) solid medium under LD conditions for 10 days in a growth chamber. Ten-day-old plants were transferred to 0.5X MS liquid medium containing 50 μM epibrassinolide (BR), 50 μM GA, 50 μM IAA, 50 μM 6-BA, 100 μM SA, 50 μM MeJA, 50 μM ABA, or 50 μM ACC. Total RNA was extracted from leaves harvested at 0 and 6 h of treatment.

4.2. Subcellular Localization

Full-length cDNA of *OsWRKY5* was amplified using gene-specific primers (**Table S1**), cloned into pCR8/GW/TOPO vector (Invitrogen), and then transferred into pEarleyGate104 (pEG104) gateway binary vector using Gateway LR clonase II enzyme mix (Invitrogen), resulting in a *35S::YFP-OsWRKY5* construct. The pEG104 vector and recombinant constructs were introduced into onion (*Allium cepa*) epidermal cells using a DNA particle delivery system (Biolistic PDS-1000/He, Bio-Rad, USA). After incubation at 25°C for 16 h, green fluorescence was detected using a confocal laser scanning microscope (SP8X, Leica, Germany). To visualize nuclei, samples were stained with 10 mL of 1 μg mL^{-1} 4`,6-diamidino-2-phenylindole dihydrochloride (DAPI) dissolved in water for 10 min then viewed using a fluorescence microscope under ultraviolet light irradiation with appropriate filters.

4.3. Determination of Photosynthetic Activity, Total Chlorophyll, and SPAD Value

To evaluate photosynthetic activity, the middle section of the flag leaf of plants grown in a paddy field under NLD conditions was adapted in the dark for 10 min. The *Fv/Fm* ratio was then measured using an OS-30p+ instrument (Opti-Sciences, USA). Total chlorophyll content was measured in rice leaves grown in the growth chamber for 4 weeks. Pigment was extracted from detached leaves incubated in complete darkness using 80% ice-cold acetone. After centrifugation

at 10,000 g for 15 min at 10°C, the absorbance of supernatants was measured at 647 nm and 663 nm using a UV/VIS spectrophotometer (BioTek Instruments, USA). The concentration of chlorophyll was calculated as previously described [55]. The change of SPAD value was determined in the flag leaf of plants grown in a paddy field under NLD conditions using a SPAD-502 instrument (KONICA MINOLTA, UK).

4.4. RT-qPCR and Stem-Loop RT-qPCR Analysis

Total RNA was extracted from rice tissues using an RNA Extraction kit (MG Med, Republic of Korea), according to the manufacturer's instructions. For synthesis of first-strand cDNA, 2 µg of total RNA was used for reverse transcription (RT) in 20 µl volume with oligo$(dT)_{15}$ primer and M-MLV reverse transcriptase (Promega). For quantification of miR164b, stem-loop pulsed RT was conducted from 2 µg of total RNA in 20 µl volume using a miR164b-specific stem-loop primer and M-MLV reverse transcriptase (Promega) with the following conditions: 16°C for 30 min followed by pulsed RT of 40 cycles at 16°C for 2 min, 42°C for 1 min, and 50°C for 1 s, and then inactivation of reverse transcription at 70°C for 5 min [56]. All RT products were diluted with 80 µl distilled water.

qPCR was performed with gene-specific primers and normalized to *UBIQUITIN5* (*UBQ5*) (Os01g22490) or rice U6 snRNA (**Table S1**) according to the $2^{-\Delta\Delta Ct}$ method [57]. The 20 µl reaction mixture included 2 µl cDNA from RT or stem-loop pulsed RT, 1 µl 0.5 µM primer, and 10 µl 2X GoTaq master mix (Promega). qPCR amplifications were conducted with a LightCycler 480 (Roche) using the following program: 94°C for 2 min followed by 40 cycles of 94°C for 15 s and 60°C for 1 min.

4.5. Yeast One-Hybrid Assays

The coding sequence of *OsWRKY5* was amplified by PCR. The PCR product was subcloned into the *Eco*RI and *Pst*I sites of pGAD424 vector (Clontech). Fragments of *OsNAP* and *OsNAC2* promoters containing the repetitive W-box core sequence (TGAC) were amplified by PCR and then cloned into pLacZi vector using *Eco*RI-*Xba*I, *Eco*RI-*Xba*I, *Sal*I-*Xho*I, *Sal*I-*Xho*I, *Sal*I-*Xho*I, *Sal*I-*Xho*I, and *Sal*I-*Xho*I sites, generating *OsNAP-1::LacZi*, *OsNAP-2::LacZi*, *OsNAC2-1::LacZi*, *OsNAC2-2::LacZi*, *OsNAC2-3::LacZi*, *OsNAC2-4::LacZi*, and *OsNAC2-5::LacZi* reporter

constructs, respectively (Clontech, USA). These vectors and empty vector were transformed into yeast strain YM4271 using the PEG/LiAc method, and yeast cells were incubated in SD/-His/-Leu liquid medium. β-Galactosidase activity was determined by absorbance of chloramphenicol red, a hydrolysis product of chlorophenol red-β-D-galactopyranoside (CPRG), at 595 nm using a UV/VIS spectrophotometer (BioTek Instruments, USA) according to the Yeast Protocol Handbook (Clontech, USA).

4.6. Determination of ABA Content

Four-week-old leaves of WT and *oswrky5-D* were pulverized in liquid nitrogen and then homogenized in 80% methanol containing 1 mM butylated hydroxytoluene as an antioxidant. Extracts incubated for 12 h at 4°C were centrifuged at 4000 *g* for 20 min. The supernatant was passed through a Sep-Pak C18 cartridge (Waters, USA) as described previously [58], and the eluate was subjected to an enzyme-linked immunosorbent assay (ELISA) using an ABA ELISA kit (MyBioSource, USA) according to the manufacturer's instructions.

5. Conclusions

We investigated a WRKY TF family member in rice, OsWRKY5, which acts as a positive regulator of ABA-induced leaf senescence. OsWRKY5 upregulates both ABA biosynthesis and transcription of CDGs and SAGs during leaf senescence, thereby promoting leaf yellowing. A negative feedback loop of ABA on *OsWRKY5* transcription contributes to maintaining ABA homeostasis during leaf senescence in rice.

Acknowledgments: This work was carried out with the support of the Cooperative Research Program for Agricultural Science & Technology Development (PJ013146), Rural Development Administration, South Korea, and the Basic Science Research Program through the National Research Foundation (NRF) of Korea funded by the Ministry of Education (NRF-2017R1A2B3003310).

Author Contributions: TK and KK performed experiments and analyzed data. KK and N-CP conceived the study, designed and supervised the project. TK, KK, and N-CP wrote and edited

the manuscript. S-HK assisted in analyzing the data. GA developed plant materials and provided advice about the manuscript. All authors read and approved the final manuscript.

Conflicts of Interest: The authors declare no conflict of interest.

Abbreviations: ABA, abscisic acid; DDI, day(s) of dark-induced senescence; DAH, day(s) after heading; NS, natural senescence; LD, long day; NLD, natural long day; DIS, dark-induced senescence; RT-qPCR, reverse transcription-quantitative PCR; CDG, chlorophyll degradation gene; SAG, senescence-associated gene; TF, transcription factor; senNAC, senescence-associated NAC gene; WT, wild-type.

References

1. Guo, Y.; Gan, S. Leaf senescence: Signals, execution, and regulation. *Curr. Top. Dev. Biol.* **2005**, 71, 83-112.
2. Lim, P.O.; Kim, H.J.; Nam, H.G. Leaf senescence. *Annu. Rev. Plant Biol.* **2007,** 58, 115-136.
3. Liu, L.; Zhou, Y.; Zhou, G.; Ye, R.; Zhao, L.; Li, X.; Lin, Y. Identification of early senescence-associated genes in rice flag leaves. *Plant Mol. Biol*. **2008,** 67, 37-55.
4. Park, S.-Y.; Yu, J.-W.; Park J.-S.; Li, J.; Yoo, S.-C.; Lee, N.-Y.; Lee, S.-K.; Jeong, S.-W.; Seo, H.S.; Koh, H.-J.; et al. The senescence-induced staygreen protein regulates chlorophyll degradation. *Plant Cell* **2007**, 19, 1649-1664.
5. Shimoda, Y.; Ito, H.; Tanaka, A. Arabidopsis *STAY-GREEN*, Mendel's green cotyledon gene, encodes magnesium-dechelatase. *Plant Cell* **2016,** 28, 2147-2160.
6. Ren, G.; An, K.; Liao, Y.; Zhou, X.; Cao, Y.; Zhao, H.; Ge, X.; Kuai, B. Identification of a novel chloroplast protein AtNYE1 regulating chlorophyll degradation during leaf senescence in Arabidopsis. *Plant Physiol*. **2007**, 144, 1429-1441.
7. Sato, Y.; Morita, R.; Nishimura, M.; Yamaguchi, H.; Kusaba, M. Mendel's green cotyledon gene encodes a positive regulator of the chlorophyll-degrading pathway. *Proc. Natl. Acad. Sci. USA* **2007**, 104, 14169-14174.
8. Barry, C.S.; McQuinn, R.P.; Chung, M.-Y.; Besuden, A.; Giovannoni, J.J. Amino acid substitutions in homologs of the STAY-GREEN protein are responsible for the *green-flesh* and *chlorophyll retainer* mutations of tomato and pepper. *Plant Physiol*. **2008**, 147, 179-187.

9. Fang, C.; Li, C.; Li, W.; Wang, Z.; Zhou, Z.; Shen Y.; Wu, M.; Wu, Y.; Li, G.; Kong, L.A.; et al. Concerted evolution of *D1* and *D2* to regulate chlorophyll degradation in soybean. *Plant J.* **2014,** 77, 700-712.

10. Morita, R.; Sato, Y.; Masuda, Y.; Nishimura, M.; Kusaba, M. Defect in non-yellow coloring 3, an α/β hydrolase-fold family protein, causes a stay-green phenotype during leaf senescence in rice. *Plant J.* **2009**, 59, 940-952.

11. Tang, Y.; Li, M.; Chen, Y.; Wu, P.; Wu, G.; Jiang H. Knockdown of *OsPAO* and *OsRCCR1* cause different plant death phenotypes in rice. *J. Plant Physiol*. **2011,** 168, 1952-1959.

12. Lee, R.-H.; Wang, C.-H.; Huang, L.-T.; Chen, S.-C.G. Leaf senescence in rice plants: cloning and characterization of senescence up-regulated genes. *J. Exp Bot*. **2001**, 52, 1117-1121.

13. Häffner, E.; Konietzki, S.; Diederichsen, E. Keeping Control: The role of senescence and development in plant pathogenesis and defense. *Plants* **2015**, 4, 449-488.

14. Piao, W.; Kim, E.-Y.; Han, S.-H.; Sakuraba, Y.; Paek, N.-C. Rice phytochrome B (OsPhyB) negatively regulates dark- and starvation-induced leaf senescence. *Plants* **2015**, 4, 644-663.

15. Rivero, R.M.; Kojima, M.; Gepstein, A.; Sakakibara, H.; Mittler, R.; Gepstein, S.; Blumwald, E. Delayed leaf senescence induces extreme drought tolerance in a flowering plant. *Proc. Natl. Acad. Sci. USA* **2007,** 104, 19631-19636.

16. Chandler. P.M.; Robertson, M. Gene expression regulated by abscisic acid and its relation to stress tolerance. *Annu. Rev. Plant Biol.* **1994**, 45, 113-141.

17. Cutler, S.R.; Rodriguez, P.L.; Finkelstein, R.R.; Abrams, S.R. Abscisic acid: Emergence of a core signaling network. *Annu. Rev. Plant Biol.* **2010,** 61, 651-679.

18. Hauser, F.; Li, Z.; Waadt, R.; Schroeder, J.I. SnapShot: Abscisic acid signaling. *Cell* **2017,** 171, 1708.e1.

19. Finkelstein, R. Abscisic acid synthesis and response. Arabdopsis Book. **2013**, 11, e0166.

20. Yang, J.; Worley, E.; Udvardi, M. A. NAP-AAO3 regulatory module promotes chlorophyll degradation via ABA biosynthesis in Arabidopsis leaves. *Plant Cell* **2014,** 26, 4862-4874.

21. Gao, S.; Gao, J.; Zhu, X.; Song, Y.; Li, Z.; Ren, G.; Zhou, X.; Kuai, B. ABF2, ABF3, and ABF4 promote ABA-mediated chlorophyll degradation and leaf senescence by transcriptional activation of chlorophyll catabolic genes and senescence-associated genes in Arabidopsis. *Mol Plant* **2016,** 9, 1272-1285.

22. Park, D.-Y.; Shim, Y.; Gi, E.; Lee, B.-D.; An, G.; Kang, K.; Paek, N.-C. The MYB-related

transcription factor RADIALIS-LIKE3 (OsRL3) functions in ABA-induced leaf senescence and salt sensitivity in rice. *Environ. Exp. Bot*. **2018,** 156, 86-95.

23. Robatzek, S.; Somssich, I.E. A new member of the *Arabidopsis* WRKY transcription factor family, AtWRKY6, is associated with both senescence-and defense-related processes. *Plant J.* **2001**, 28, 123-133.
24. Zhang, K.; Gan, S.-S. An Abscisic Acid-AtNAP Transcription factor SAG113 protein phosphatase 2C regulatory chain for controlling dehydration in senescing Arabidopsis leaves. *Plant Physiol*. **2012**, 158, 961-969.
25. Liang, C.; Wang, Y.; Zhu, Y.; Tang, J.; Hu, B.; Liu, L.; Ou, S.; Wu, H.; Sun, X.; Chu, J.; et al. OsNAP connects abscisic acid and leaf senescence by fine-tuning abscisic acid biosynthesis and directly targeting senescence-associated genes in rice. *Proc. Natl. Acad. Sci. USA* **2014,** 111, 10013-10018.
26. Rushton, P.J.; Somssich, I.E.; Ringler, P.; Shen, Q.J. WRKY transcription factors. *Trends Plant Sci.* **2010**, 15, 247-258.
27. Guo, Y.; Cai, Z.; Gan, S. Transcriptome of Arabidopsis leaf senescence. *Plant Cell Environ*. **2004**, 27, 521-549.
28. Liu, L.; Xu, W.; Hu, X.; Liu, H.; Lin, Y. W-box and G-box elements play important roles in early senescence of rice flag leaf. *Sci. Rep*. **2016**, 6, 20881.
29. Robatzek, S.; Somssich, I.E. Targets of *At*WRKY6 regulation during plant senescence and pathogen defense. *Genes Dev*. **2002,** 16, 1139-1149.
30. Miao, Y.; Laun, T.; Zimmermann, P.; Zentgraf, U. Targets of the WRKY53 transcription factor and its role during leaf senescence in Arabidopsis. *Plant Mol. Biol*. **2004**, 55, 853-867.
31. Zhou, X.; Jiang, Y.; Yu, D. WRKY22 transcription factor mediates dark-induced leaf senescence in Arabidopsis. *Mol. Cells* **2011**, 31, 303-313.
32. Besseau, S.; Li, J.; Palva, E.T. WRKY54 and WRKY70 co-operate as negative regulators of leaf senescence in Arabidopsis thaliana. *J. Exp. Bot.* **2012,** 63, 2667-2679.
33. Chen, L.; Xiang, S.; Chen, Y.; Li, D.; Yu, D. *Arabidopsis* WRKY45 interacts with the DELLA protein RGL1 to positively regulate age-triggered leaf senescence. *Mol. Plant* **2017**, 10, 1174-1189.
34. Guo, P.; Li, Z.; Huang, P.; Li, B.; Fang, S.; Chu, J.; Guo, H. A tripartite amplification loop involving the transcription factor WRKY75, salicylic acid, and reactive oxygen species

accelerates leaf senescence. *Plant Cell* **2017,** 29, 2854-2870.

35. Jing, S.; Zhou, X.; Song, Y.; Yu, D. Heterologous expression of *OsWRKY23* gene enhances pathogen defense and dark-induced leaf senescence in Arabidopsis. *Plant Growth Regul.* **2009,** 58, 181-190.
36. Han, M.; Kim, C.-Y.; Lee, J.; Lee, S.-K.; Jeon, J.-S. *OsWRKY42* represses *OsMT1d* and induces reactive oxygen species and leaf senescence in Rice. *Mol. Cells* **2014,** 37, 532-539.
37. Eulgem, T.; Rushton, P.J.; Robatzek, S.; Somssich, I.E. The WRKY superfamily of plant transcription factors. *Trends Plant Sci*. **2000,** 5, 199-206.
38. Netto, A.T.; Campostrini, E.; de Oliveira, J.G.; Bressan-Smith, R.E. Photosynthetic pigments, nitrogen, chlorophyll *a* fluorescence and SPAD-502 readings in coffee leaves. *Sci. Hort.* **2005**, 104, 199-209.
39. Sim, C.C.; Zaharah, A.R.; Tan, M.S.; Goh, K.J. Rapid determination of leaf chlorophyll concentration, photosynthetic activity and NK concentration of Elaies guineensis via correlated SPAD-502 chlorophyll index. *Asian J. Agric. Res.* **2015**, 9, 132-138.
40. Mao, C.; Lu, S.; Lv, B.; Zhang, B.; Shen, J.; He, J.; Luo, L.; Xi, D.; Chen, X.; Ming, F. A rice NAC transcription factor promotes leaf senescence via ABA biosynthesis. *Plant Physiol.* **2017**, 174, 1747-1763.
41. Ciolkowski, I.; Wanke, D.; Birkenbihi, R.P.; Somssich, I.E. Studies on DNA-binding selectivity of WRKY transcription factors lend structural clues into WRKY-domain function. *Plant Mol. Biol*. **2008,** 68, 81-92.
42. Fang, Y.; Xie, K.; Xiong, L. Conserved miR164-targeted NAC genes negatively regulate drought resistance in rice. *J. Exp. Bot*. **2014**, 65, 2119-2135.
43. Jiang, D.; Chen, W.; Dong, J.; Li, J.; Yang, F.; Wu, Z.; Zhou, H.; Wang, W.; Zhuang, C. Overexpression of miR164b-resistant *OsNAC2* improves plant architecture and grain yield in rice. *J. Exp. Bot*. **2018**, 69, 1533-1543.
44. Zhang, H.; Zhou, C. Signal transduction in leaf senescence. *Plant Mol. Biol*. **2013**, 82, 539-545.
45. Gu, L.; Dou, L.; Guo, Y.; Wang, H.; Li, L.; Wang, C.; Ma, L.; Wei, H.; Yu, S. The WRKY transcription factor *GhWRKY27* coordinates the senescence regulatory pathway in upland cotton (Gossypium hirsutum L.). *BMC Plant Biol*. **2019**, 19, 116.
46. Noodén, L.D. Abscisic acid, auxin, and other regulators of senescence. In: Noodén LD,

519 Leopold AC, editors. Senescence and aging in plants. San Diego: Academic Press; **1988,**
520 p.329–355.
521 47. Breeze, E.; Harrison, E.; McHattie, S.; Hughes, L.; Hickman, R.; Hill, C.; Kiddle, S.; Kim,
522 Y.-S.; Penfold, C.A.; Jenkins, D.; et al. High-resolution temporal profiling of transcripts
523 during Arabidopsis leaf senescence reveals a distinct chronology of processes and regulation.
524 *Plant Cell* **2011**, 23, 873-894.
525 48. van der Graaff, E.; Schwacke, R.; Schneider, A.; Desimone, M.; Flügge, U.-I.; Kunze, R.
526 Transcription analysis of Arabidopsis membrane transporters and hormone pathways during
527 developmental and induced leaf senescence. *Plant Physiol*. **2006,** 141, 776-792.
528 49. Huang, Y.; Guo, Y.; Liu, Y.; Zhang, F.; Wang, Z.; Wang, H.; Wang, F.; Li, D.; Mao, D.;
529 Luan, S.; et al. 9-*cis*-Epoxycarotenoid dioxygenase 3 regulates plant growth and enhances
530 multi-abiotic stress tolerance in rice. *Front. Plant Sci*. **2018**, 9, 162.
531 50. Ren, T.; Wang, J.; Zhao, M.; Gong, X.; Wang, S.; Wang, G.; Zou, C. Involvement of NAC
532 transcription factor SiNAC1 in a positive feedback loop via ABA biosynthesis and leaf
533 senescence in foxtail millet. *Planta* **2018,** 247, 53-68.
534 51. Rushton, D.L.; Tripathi, P.; Rabara, R.C.; Lin, J.; Ringler, P.; Boken, A.K.; Langum, T.J.;
535 Smidt, L.; Boomsma, D.D.; Emme, N.J.; et al. WRKY transcription factors: key components
536 in abscisic acid signaling. *Plant Biotechnol. J.* **2012,** 10, 2-11.
537 52. Ma, X.; Zhang, Y.; Turečková, V.; Xue, G.-P.; Fernie, A.R.; Mueller-Roeber, B.; Balazadeh,
538 S. The NAC transcription factor SlNAP2 regulates leaf senescence and fruit yield in tomato.
539 *Plant Physiol*. **2018,** 177, 1286-1302.
540 53. Jeon, J.-S.; Lee, S.; Jung, K.-H.; Jun, S.-H.; Jeong, D.-H.; Lee, J.; Kim, C.; Jang, S.; Yang,
541 K.; Nam, J.; et al. T-DNA insertional mutagenesis for functional genomics in rice. *Plant J.*
542 **2000**, 22, 561-570.
543 54. Jeong, D.-H.; An, S.; Park, S.; Kang, H.-G.; Park, G.-G.; Kim, S.-R.; Sim, J.; Kim, Y.O.;
544 Kim, M.K.; Kim, S.R.; et al. Generation of a flanking sequence-tag database for activation-
545 tagging lines in japonica rice. *Plant J*. **2006,** 45, 123-132.
546 55. Porra, R.J. Thompson WA, Kriedemann PE. Determination of accurate extinction
547 coefficients and simultaneous equations for assaying chlorophylls a and b extracted with four
548 different solvents: verification of the concentration of chlorophyll standards by atomic
549 absorption spectroscopy. *Biochim. Biophys. Acta BBA - Bioenerg*. **1989,** 975, 384-394.

550 56. Varkonyi-Gasic, E.; Wu, R.; Wood, M.; Walton, E.F.; Hellens, R.P. Protocol: a highly
551 sensitive RT-PCR method for detection and quantification of microRNAs. *Plant Methods*.
552 **2007,** 3, 12.
553 57. Livak, K.J.; Schmittgen, T.D. Analysis of relative gene expression data using real-time
554 quantitative PCR and the $2^{-\Delta\Delta C_T}$ method. *Methods*. **2001,** 25, 402-408.
555 58. Yang, J.; Zhang, J.; Wang, Z.; Zhu, Q.; Wang, W. Hormonal changes in the grains of rice
556 subjected to water stress during grain filling. *Plant Physiol*. **2001**, 127, 315-323.
557

Preprints (www.preprints.org) | NOT PEER-REVIEWED | Posted: 18 August 2019 doi:10.20944/preprints201908.0189.v1

Peer-reviewed version available at Int. J. Mol. Sci. 2019, 20, 4437; doi:10.3390/ijms20184437

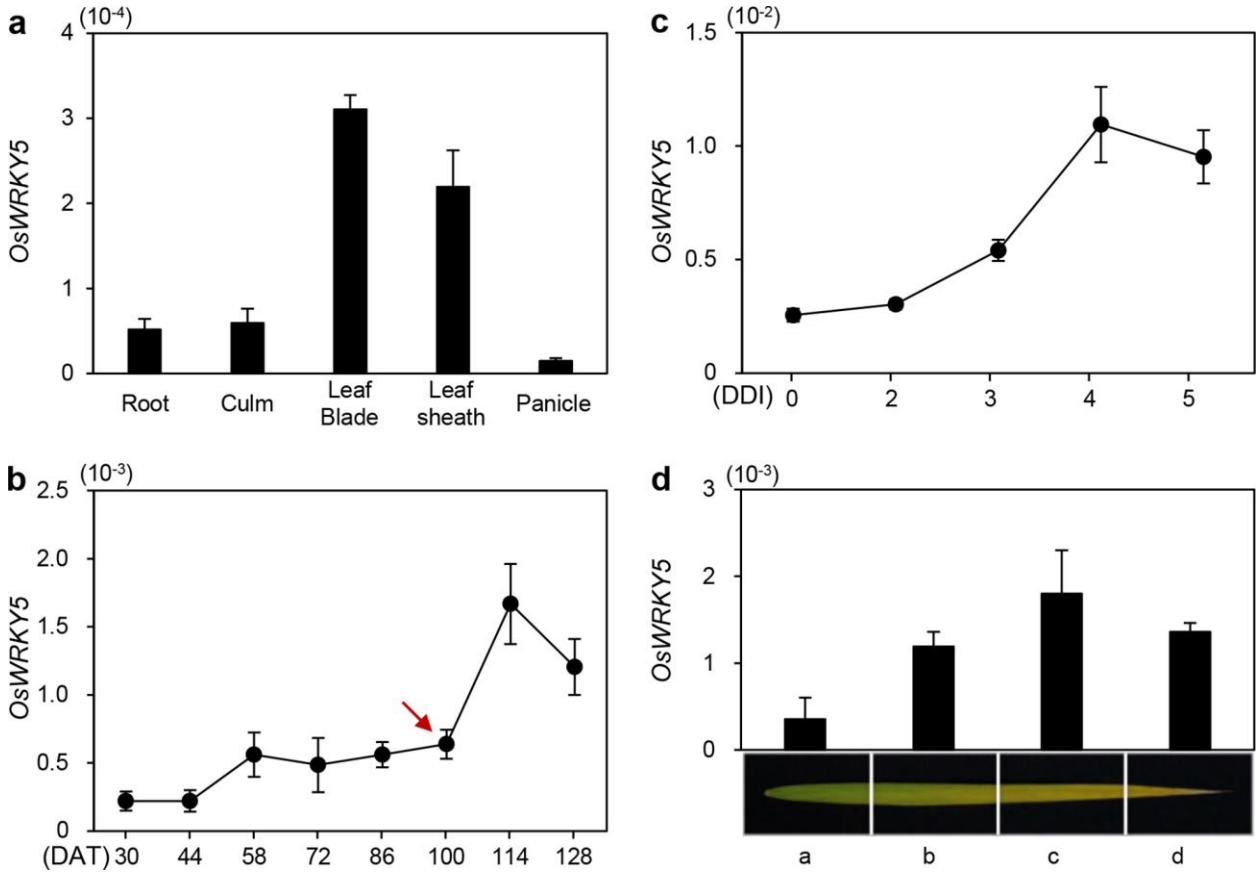

Figure 1. Expression profiles of *OsWRKY5* in rice

(**a**) *OsWRKY5* mRNA levels in detached organs from the *japonica* cultivar 'Dongjin' (hereafter wild type; WT) at the heading stage. *OsWRKY5* was mainly expressed in leaf blade and leaf sheath. (**b, c**) Changes in *OsWRKY5* expression level in leaf blades of WT rice grown in a paddy field (**b**) or in the greenhouse (**c**) under natural long day conditions (≥14 h light/day). Red arrow indicates heading date. (**d**) Expression of *OsWRKY5* measured in flag leaves divided into four regions from the green sector (a) to the yellow sector (d) at 128 days after transplanting (DAT). *OsWRKY5* mRNA levels were determined by RT-qPCR analysis and normalized to that of *OsUBQ5* (Os01g22490). Mean and SD values were obtained from at least three biological samples. Experiments were repeated twice with similar results. DDI, day(s) of dark incubation.

Preprints (www.preprints.org) | NOT PEER-REVIEWED | Posted: 18 August 2019 doi:10.20944/preprints201908.0189.v1

Peer-reviewed version available at Int. J. Mol. Sci. 2019, 20, 4437; doi:10.3390/ijms20184437

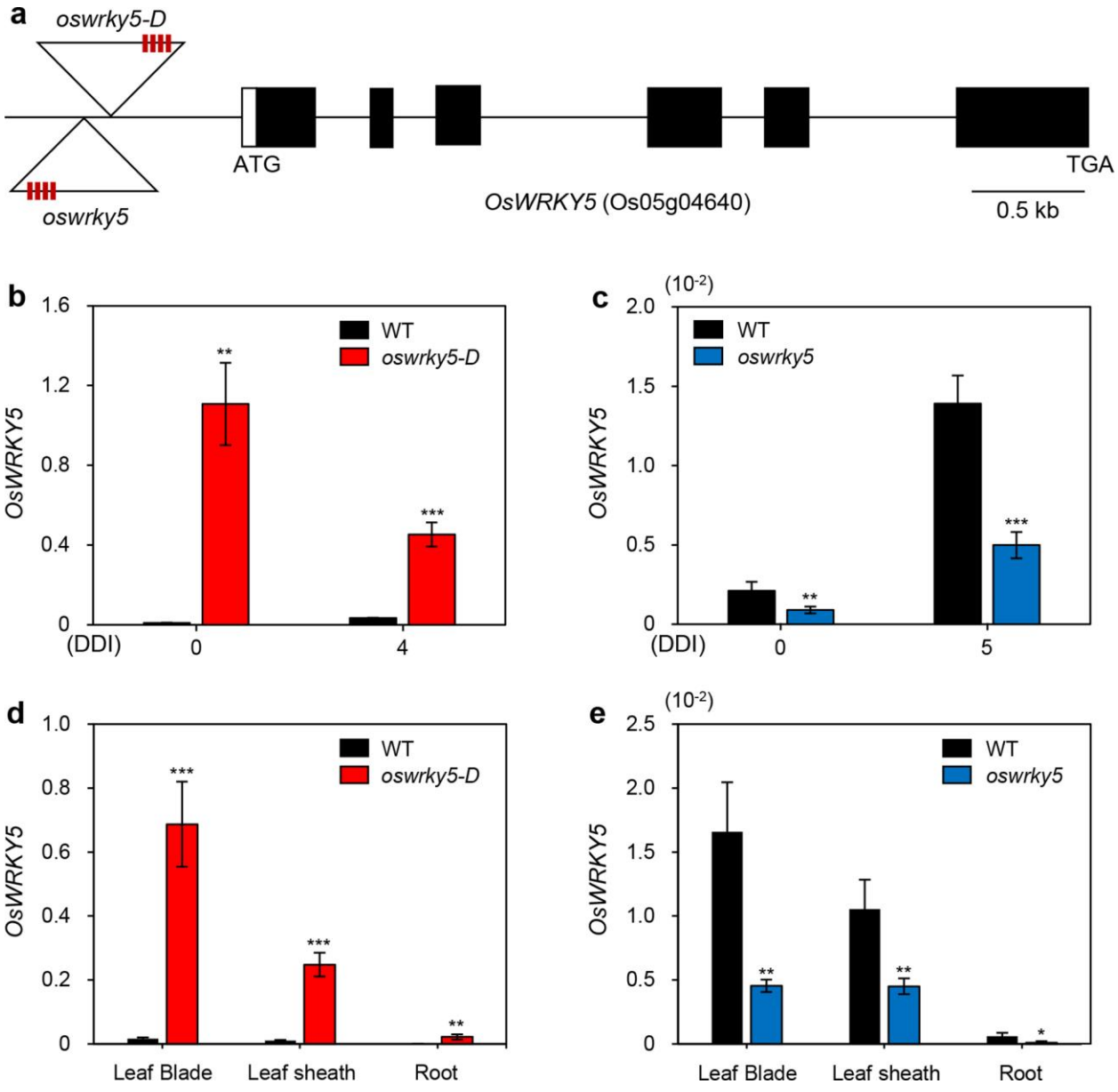

Figure 2. Mutation of *OsWRKY5* by T-DNA insertion.

(**a**) Schematic diagram depicting the positions of T-DNA insertions in the promoter region of *OsWRKY5* (LOC_Os05g04640). Black and white bars represent exons and 5′-untranslated region, respectively. Open triangles indicate the location of the *OsWRKY5* T-DNA insertions (*oswrky5-D*, PFG_3A-15928; *oswrky5*, PFG_3A-06060). Red boxes on triangles represent tetramerized 35S enhancers (4× 35S). (**b**, **c**) Total RNA was isolated from detached leaves of WT and mutant lines (*oswrky5-D* and *oswrky5*) under DIS as shown in Figure 3a and 3b. (**d**, **e**) *OsWRKY5* mRNA levels were measured in rice tissues separated from three-week-old WT and

mutant lines. Transcript levels of *OsWRKY5* in *oswrky5-D* (**b**, **d**) and *oswrky5* (**c**, **e**) were determined by RT-qPCR and normalized to the transcript levels of *OsUBQ5*. Mean and SD values were obtained from more than three biological replicates. Asterisks indicate a statistically significant difference from WT, as determined by Student's *t*-test (**P* < 0.05, ***P* < 0.01, ****P* < 0.001). DDI, day(s) of dark incubation.

Preprints (www.preprints.org) | NOT PEER-REVIEWED | Posted: 18 August 2019 doi:10.20944/preprints201908.0189.v1

Peer-reviewed version available at Int. J. Mol. Sci. 2019, 20, 4437; doi:10.3390/ijms20184437

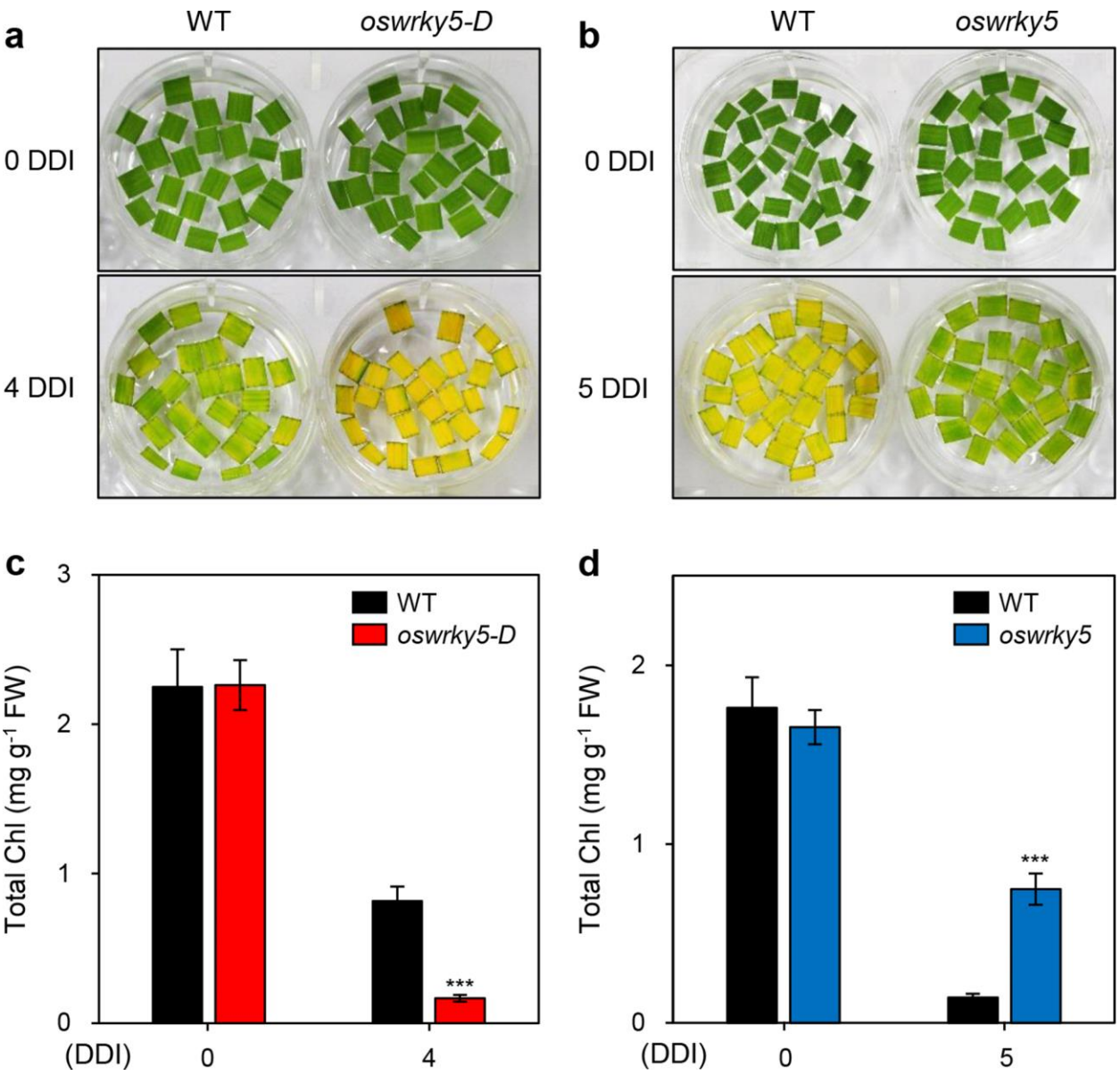

Figure 3. *OsWRKY5* promotes leaf yellowing under DIS conditions.

WT and mutant lines (*oswrky5-D* and *oswrky5*) were grown in paddy soil for four weeks under natural long day conditions (≥14 h light/day). (**a, b**) Yellowing of detached leaves induced in 3 mM MES buffer (pH 5.8) at 28°C under complete darkness. Changes in leaf color (**a, b**) and total chlorophyll (Chl) contents (**c, d**) of *oswrky5-D* or *oswrky5* mutants compared with the WT after 4 or 5 days of dark incubation (DDI), respectively. Mean and SD values were obtained from more than three biological replicates. Asterisks indicate a statistically significant difference from WT, as determined by Student's *t*-test (***$P < 0.001$). Experiments were repeated twice with similar results. FW, fresh weight.

Preprints (www.preprints.org) | NOT PEER-REVIEWED | Posted: 18 August 2019 doi:10.20944/preprints201908.0189.v1

Peer-reviewed version available at Int. J. Mol. Sci. 2019, 20, 4437; doi:10.3390/ijms20184437

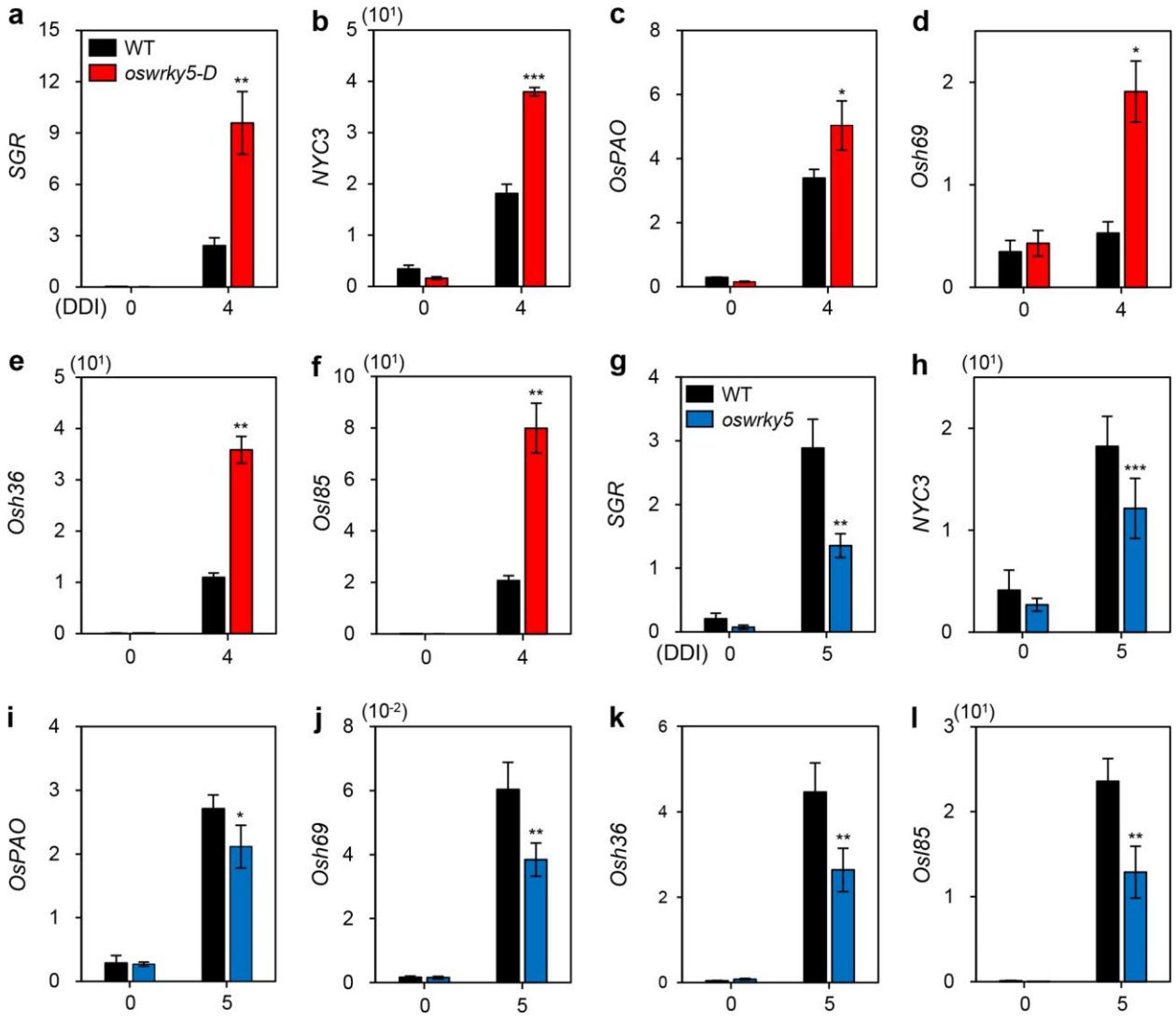

Figure 4. Altered expression of CDGs and SAGs in *oswrky5-D* and *oswrky5* during DIS. Total RNA was isolated from detached leaves of WT and mutant lines (*oswrky5-D* and *oswrky5*) under DIS as shown in Fig. 2(a, b). Expression of CDGs and SAGs in *oswrky5-D* (**a–f**) or *oswrky5* (**g–l**) was compared with that in the WT after 4 or 5 DDI, respectively. Transcript levels of CDGs (**a–c** and **g–i**) and SAGs (**d–f** and **j–l**) were determined by RT-qPCR analysis and normalized to that of *OsUBQ5*. Mean and SD values were obtained from more than three biological replicates. Asterisks indicate a statistically significant difference from WT, as determined by Student's *t*-test (**P* < 0.05, ***P* < 0.01, ****P* < 0.001). Experiments were repeated twice with similar results. CDGs, Chl degradation genes; DDI, day(s) of dark incubation; SAGs, senescence-associated genes.

Preprints (www.preprints.org) | NOT PEER-REVIEWED | Posted: 18 August 2019 doi:10.20944/preprints201908.0189.v1

Peer-reviewed version available at Int. J. Mol. Sci. 2019, 20, 4437; doi:10.3390/ijms20184437

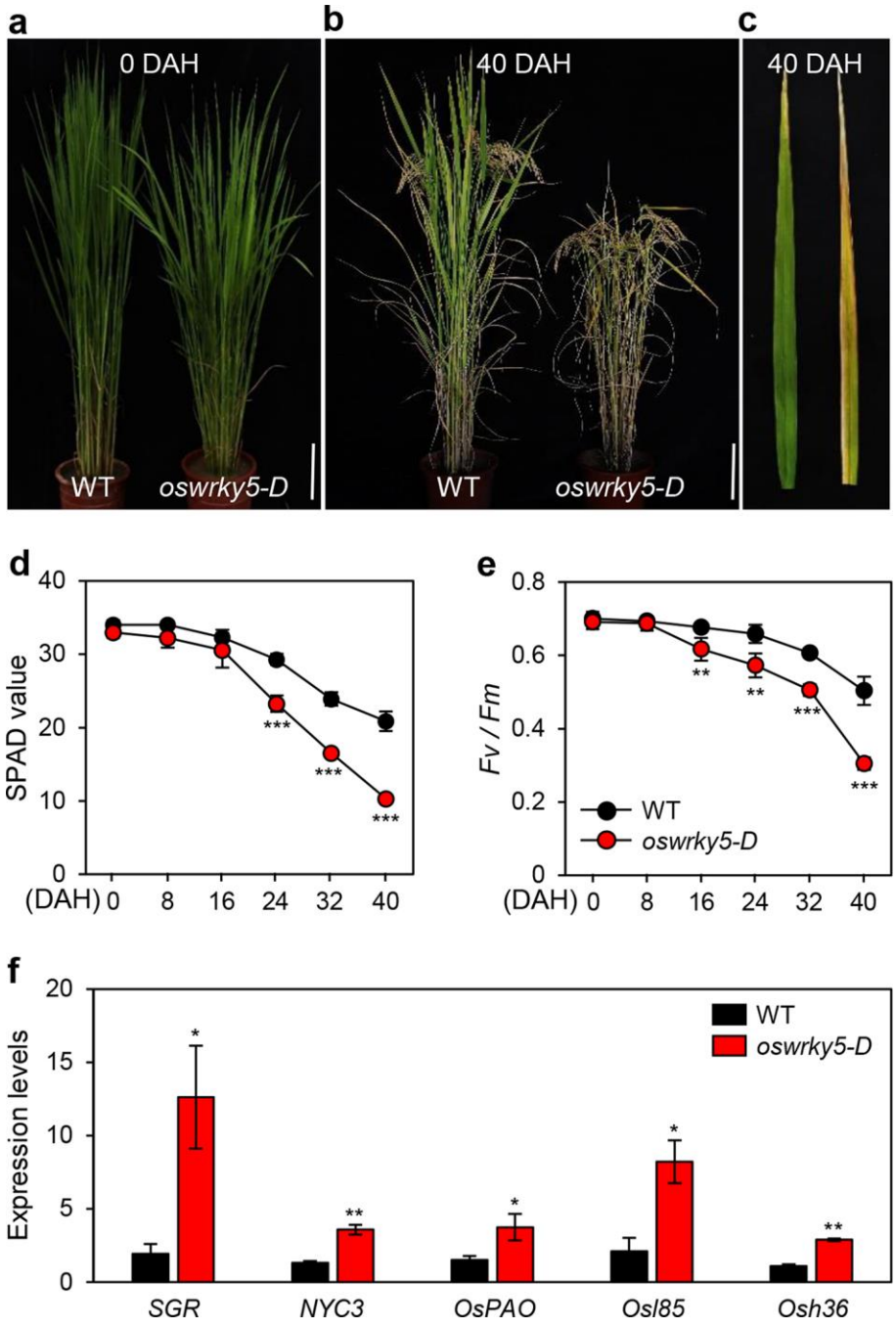

Figure 5. *oswrky5-D* promotes leaf senescence during NS.

WT and *oswrky5-D* plants were grown in a paddy field under natural long-day conditions (≥14 h light/day). (**a, b**) Phenotypes of WT and *oswrky5-D* plants at heading (0 DAH) (**a**) and 40 days after heading (DAH) (**b**). White scale bars = 20 cm. (**c**) Senescing flag leaves of WT (*left*) and *oswrky5-D* (*right*) at 40 DAH. Photos shown are representative of five independent plants. (**d–e**) Changes in SPAD value (**d**) and photosystem II (PSII) activity (*Fv/Fm*) (**e**) in flag leaves at

heading. (**f**) Expression of CDGs and SAGs measured in senescing flag leaves (**c**). Transcript levels were determined by RT-qPCR analysis and normalized to that of *OsUBQ5*. Mean and SD values were obtained from more than three biological replicates. Asterisks indicate a statistically significant difference from WT, as determined by Student's *t*-test (*$P < 0.05$, **$P < 0.01$, ***$P < 0.001$).

Preprints (www.preprints.org) | NOT PEER-REVIEWED | Posted: 18 August 2019 doi:10.20944/preprints201908.0189.v1

Peer-reviewed version available at Int. J. Mol. Sci. 2019, 20, 4437; doi:10.3390/ijms20184437

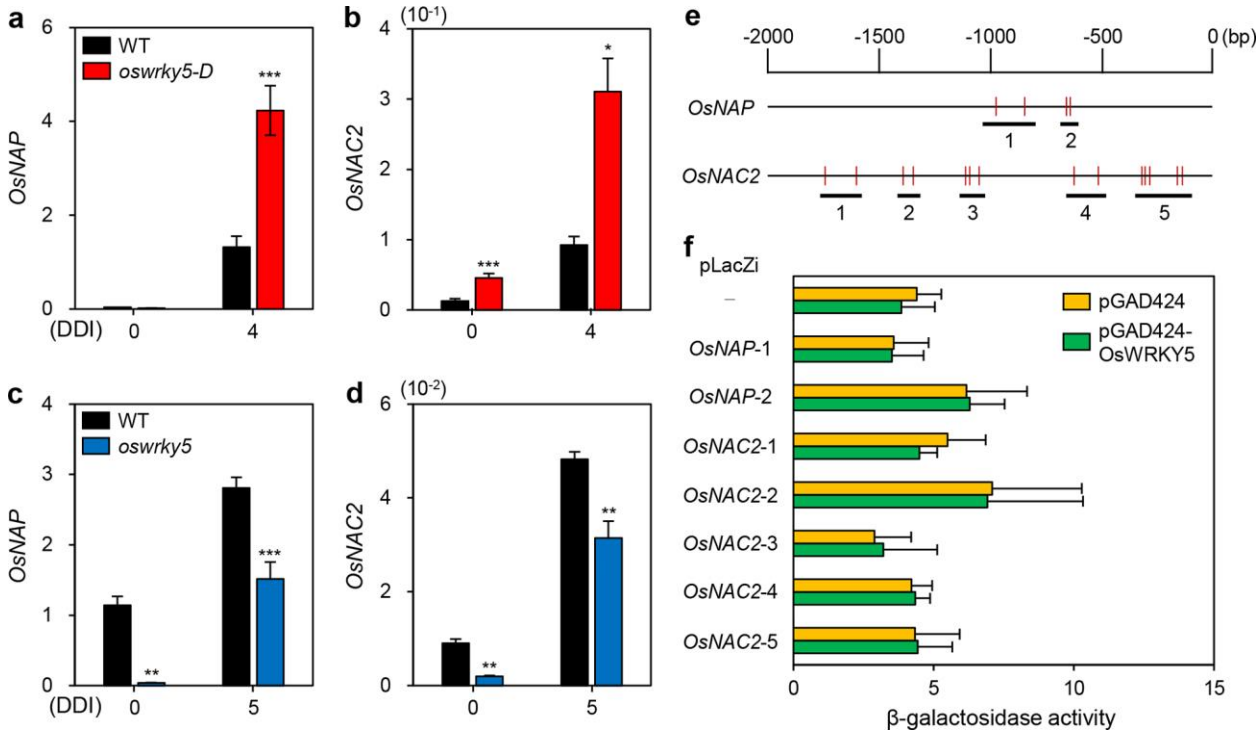

Figure 6. OsWRKY5 indirectly regulates expression of senescence-induced NAC TFs. (**a–d**) Total RNA was isolated from detached leaves of WT and mutant lines (*oswrky5-D* and *oswrky5*), as shown in Figure 2(a, b). Transcript levels of *OsNAP* (**a, c**) and *OsNAC2* (**b, d**) were determined by RT-qPCR analysis and normalized to the transcript levels of *OsUBQ5*. Mean and SD values were obtained from more than three biological replicates. Asterisks indicate a statistically significant difference from WT, as determined by Student's *t*-test (**P* < 0.05, ***P* < 0.01, ****P* < 0.001). (**e, f**) Interaction of OsWRKY5 with the promoters of *OsNAP* and *OsNAC2* by yeast one-hybrid assays. (**e**) Numbers represent upstream base pairs from the transcriptional initiation sites of *OsNAP* and *OsNAC2*. Vertical red lines represent the W-box core sequence (TGAC). Horizontal black bars represent regions containing repetitive TGAC sequences. (**f**) β-Galactosidase activity of bait plasmids (pGAD424 and pGAD424-OsWRKY5) evaluated by the absorbance of chloramphenicol red, a hydrolysis product of chlorophenol red-β-D-galactopyranoside (CPRG). Empty bait (pGAD424) and prey plasmids (-) were used for negative controls. Experiments were repeated twice with similar results. DDI, day(s) of dark incubation.

Preprints (www.preprints.org) | NOT PEER-REVIEWED | Posted: 18 August 2019 doi:10.20944/preprints201908.0189.v1

Peer-reviewed version available at Int. J. Mol. Sci. 2019, 20, 4437; doi:10.3390/ijms20184437

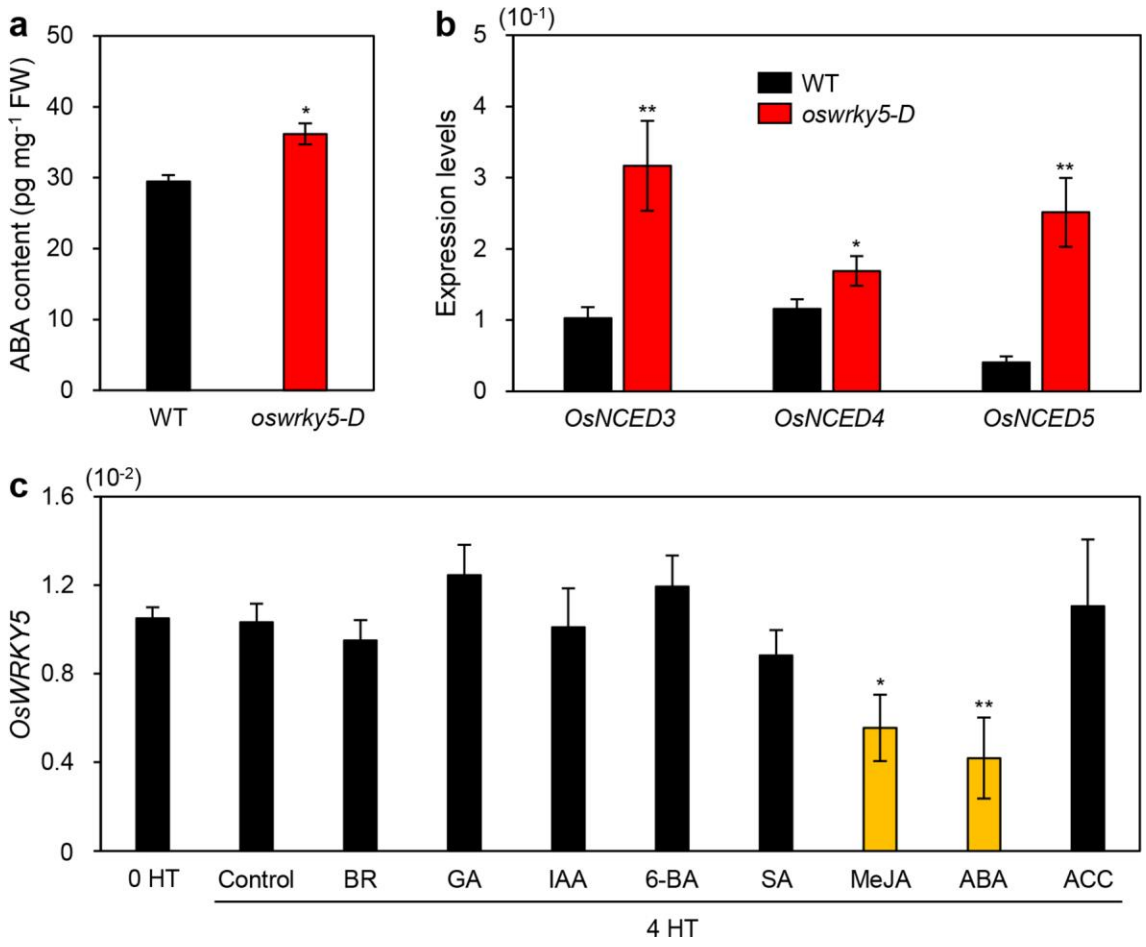

Figure 7. *OsWRKY5* participates in ABA-mediated senescence pathways. (**a**) Endogenous ABA contents measured in leaves of WT and *oswrky5-D* plants grown in paddy soil for 3 weeks under LD conditions. FW, fresh weight. (**b**) Total RNA was extracted from leaves of the same WT and *oswrky5-D* plants used for the analysis shown in Figure 6A. Transcript levels of ABA biosynthetic genes including *OsNCED3*, *OsNCED4*, and *OsNCED5* were determined by RT-qPCR analysis and normalized to transcript levels of *OsUBQ5*. Mean and SD values were obtained from more than three biological replicates. Asterisks indicate a statistically significant difference from WT, as determined by Student's *t*-test (*$P < 0.05$, **$P < 0.01$). (**c**) Ten-day-old WT seedlings grown on 0.5X MS phytoagar medium at 28°C under continuous light conditions were transferred to 0.5X MS liquid medium only (control) or 0.5X MS liquid medium containing 50 μM epibrassinolide (BR), 50 μM gibberellic acid (GA), 50 μM 3-indoleacetic acid (IAA), 50 μM 6-benzylaminopurine (6-BA), 100 μM salicylic acid (SA), 50 μM methyl jasmonic acid (MeJA), 50 μM abscisic acid (ABA), or 50 μM 1-aminocyclopropane-

1-carboxylic acid (ACC). Total RNA was isolated from leaves after 4 h of treatment. *OsWRKY5* mRNA levels were determined by RT-qPCR analysis and normalized to transcript levels of *OsUBQ5*. Mean and SD values were obtained from more than three biological replicates. Asterisks on orange bars indicate a statistically significant difference from the control, as determined by Student's *t*-test (*$P < 0.05$, **$P < 0.01$). Experiments were repeated twice with similar results.

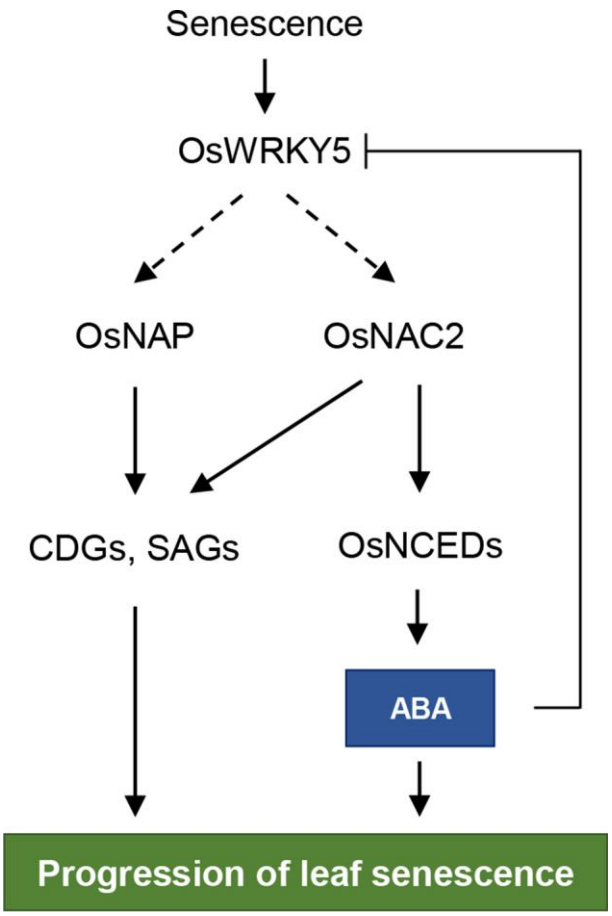

Figure 8. Proposed model for the role of OsWRKY5 in leaf senescence. Arrows indicate activation and bar-ended line represents inhibition. Solid and dashed arrows represent direct and indirect regulation, respectively.